

# Simulated responses of cerebellar Purkinje cells are independent of the dendritic location of granule cell synaptic inputs

(cerebellum/amplification/parallel fiber/calcium channel/model)

ERIK DE SCHUTTER\*† AND JAMES M. BOWER

Division of Biology 216-76, California Institute of Technology, Pasadena, CA 91125

Communicated by John J. Hopfield, February 3, 1994

**ABSTRACT** Cerebellar Purkinje cell responses to granule cell synaptic inputs were examined with a computer model including active dendritic conductances. Dendritic P-type  $\text{Ca}^{2+}$  channels amplified postsynaptic responses when the model was firing at a physiological rate. Small synchronous excitatory inputs applied distally on the large dendritic tree resulted in somatic responses of similar size to those generated by more proximal inputs. In contrast, in a passive model the somatic postsynaptic potentials to distal inputs were 76% smaller. The model predicts that the somatic firing response of Purkinje cells is relatively insensitive to the exact dendritic location of synaptic inputs. We describe a mechanism of  $\text{Ca}^{2+}$ -mediated synaptic amplification, based on the subspiking threshold recruitment of P-type  $\text{Ca}^{2+}$  channels in the dendritic branches surrounding the input site.

The interaction between the geometry of a neuron's dendrite and how that neuron processes synaptic information is a central question in neurobiology. Theoretical analysis by Rall (1) and others (2) has shown that in large dendritic trees, synaptic inputs on distal locations will be attenuated much more than inputs on proximal branches before they arrive at the soma. A generally accepted conclusion from these studies is that the exact dendritic location of synaptic inputs is quite important (3). However, this analysis is based on the assumption of a passive dendritic membrane.

The cerebellar Purkinje cell has a large dendritic tree (4), covered with an enormous number of excitatory parallel fiber synapses (5). The geometry of the cerebellar molecular layer is such that parallel fibers make synapses at similar vertical positions in all Purkinje cells they contact (4). Thus, if distal synaptic inputs are attenuated in Purkinje cells, parallel fibers at the top of the molecular layer should have little influence on Purkinje cell somatic responses. Because Purkinje cells generate the only output from the cerebellar cortex (6), this would effectively mean that many granule cells have little effect on cerebellar output.

However, Purkinje cells are known to generate prominent dendritic  $\text{Ca}^{2+}$  currents in response to synaptic inputs (6–8). Because increases in membrane conductance also increase the electrotonic length of dendrites, the presence of active channels on the Purkinje cell dendrite and the continuous background synaptic input from the parallel fibers could both be expected to further enhance synaptic attenuation (9–11). In this paper, we use a Purkinje cell model (11, 12) to show that the active properties of the dendrite actually interact with the background synaptic input and with the passive electrical properties of the cell to amplify distal synaptic inputs, effectively negating the significance of dendritic location. Our modeling results suggest that in Purkinje cells all granule cell inputs have equal access to the soma independent

of their spatial position. If correct, this result has profound implications for the nature of information processing within the cerebellar cortex.

## MODEL AND METHODS

All simulations used a detailed compartmental model of a Purkinje cell based on reconstructed dendritic anatomy (13). The model was simulated with GENESIS (14) and has been described in detail elsewhere (11, 12). Purkinje cell morphology and dendritic spines were modeled using 4588 compartments. In the full model, all dendritic compartments, except those representing spines, contained P-type (15) and T-type (16)  $\text{Ca}^{2+}$  channels, two different  $\text{Ca}^{2+}$ -activated  $\text{K}^{+}$  channels (17), and a persistent  $\text{K}^{+}$  channel; the soma contained a fast and a persistent  $\text{Na}^{+}$  channel (8), delayed rectifier, A current, persistent  $\text{K}^{+}$  channel, and anomalous rectifier. In several simulations (see Figs. 1–3) the soma was completely passive so that a somatic excitatory postsynaptic potential (EPSP) could be recorded. The active membrane model was also compared with a completely passive model that had an identical morphology and the same leak conductance.

This model has been shown to replicate current injection data *in vitro* (11) and to generate appropriate responses to synaptic inputs by climbing fibers, parallel fibers, and inhibitory neurons (12). The model shows spontaneous firing patterns similar to those seen in Purkinje cells *in vivo* (18) when asynchronous excitation, representing parallel fiber inputs, is combined with asynchronous inhibition from stellate cells (12). All the results presented in this paper, except Table 1, were obtained with random excitation at 28 Hz and asynchronous inhibition at 1 Hz, which in the full model resulted in an average firing rate of 66 Hz. (See ref. 12 for the physiological relevance of the frequency of excitation.)

The sensitivity of the model to localized synaptic inputs was tested by giving small synchronous excitatory inputs (time to peak, 0.8 ms; 0.7 nS) on 200 spines. These spines were put on dendritic branches with a diameter of  $<1.5 \mu\text{m}$ , which corresponds to the location of ascending branch synapses (18, 19). For computational efficiency, only 20 spines (instead of 200) with a peak synaptic conductance of 7 nS were used in some simulations (in Figs. 2 and 5 and Table 1). Control simulations with all 200 spines showed that this simplification had no effect on results.

Amplification was calculated as the ratio of the peak EPSP amplitude in the active model over the amplitude in the passive model.

## RESULTS

Identical synchronous synaptic inputs were provided on various branchlets of the dendrite in active and passive

The publication costs of this article were defrayed in part by page charge payment. This article must therefore be hereby marked "advertisement" in accordance with 18 U.S.C. §1734 solely to indicate this fact.

Abbreviation: EPSP, excitatory postsynaptic potential.

\*Present address: Born Bunge Foundation, University of Antwerp, 2610 Antwerp, Belgium.

†To whom reprint requests should be addressed.

membrane models of a Purkinje cell and the somatic EPSPs were compared (Fig. 1). The inputs were restricted to single branchlets to make comparisons between different locations easier, even though actual synchronous inputs are probably more dispersed.

EPSPs in the active model were larger than the EPSP in the passive model for all regions of the dendrite. Thus, ionic channels in the dendrite amplified all synaptic inputs. EPSPs in the active model also showed less variation of amplitude (SD, 34%;  $n = 12$ ) compared to the passive model (SD, 61%). In the passive model, peak somatic EPSP amplitude decreased with distance of the input and was 76% smaller for distal than for proximal inputs. In the active model near and far inputs produced similar somatic EPSP sizes (Fig. 1). Synaptic inputs in the active model were thus amplified differentially, with distal synaptic inputs more affected than proximal ones. The variability of the EPSP amplitude in the active model was related to intrinsic variations in the size of the input branchlets—i.e., inputs on small distal branchlets caused smaller EPSPs than inputs on large branchlets.

The amplification of the somatic EPSP was linearly related to input distance from the soma for distances beyond 100  $\mu\text{m}$  from the soma (Fig. 2). This relative amplification of distal inputs was not caused by a big increase of the EPSP amplitude at the location of the input, as the amplification of EPSPs in the spine heads was very small and not related to distance (Fig. 2). This is demonstrated in more detail in Fig. 3, which compares EPSPs in the spine heads of the active and passive membrane models for a proximal input (Fig. 3A) and a distal input (Fig. 3B). In the passive membrane model, EPSP amplitudes in spine heads on proximal dendrites ( $27.0 \pm 1.0$  mV) were smaller than those on distal dendrites ( $41.6 \pm 3.0$  mV). This was caused by a current sink effect (2) due to the large, leaky soma. In the spines on distal dendrites, the peak amplitudes of the EPSPs in the passive and active membrane models were almost identical (Fig. 3B), confirming that the

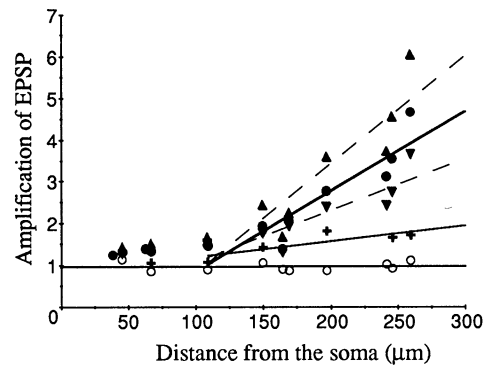


FIG. 2. Amplification of somatic EPSPs (●) and of EPSPs in the spine heads (○) in the standard model vs. distance from the soma. Effect of parameter changes on the amplification of somatic EPSPs is also shown: a 10% decrease in the density of dendritic P channels (▼), a 10% increase in density (▲), and a shift of the P-channel activation threshold to  $-35$  mV (+). Amplification of the somatic EPSPs was positively correlated with distance beyond 100  $\mu\text{m}$  (thick line, standard model; broken lines, changes in P-channel density); linear correlation coefficients were 0.85–0.91. There was no correlation between distance and amplification in the spine heads. All data points are the average of 40 events; distance was measured along the smooth dendrites from the root of the input branchlet to the soma.

amplification of distal inputs did not occur at the site of the input. However, the EPSPs in the spine heads of the active membrane model consisted of two parts everywhere. An initial rapid increase that overlapped the passive EPSP was followed by a slower depolarization. This second component was a small, localized  $\text{Ca}^{2+}$  spike caused by activation of dendritic P-type  $\text{Ca}^{2+}$  channels (15).

The larger amplification of distal inputs resulted from an interaction between the electronic structure of the neuron and P-channel activation, which is illustrated in Fig. 4. Distal

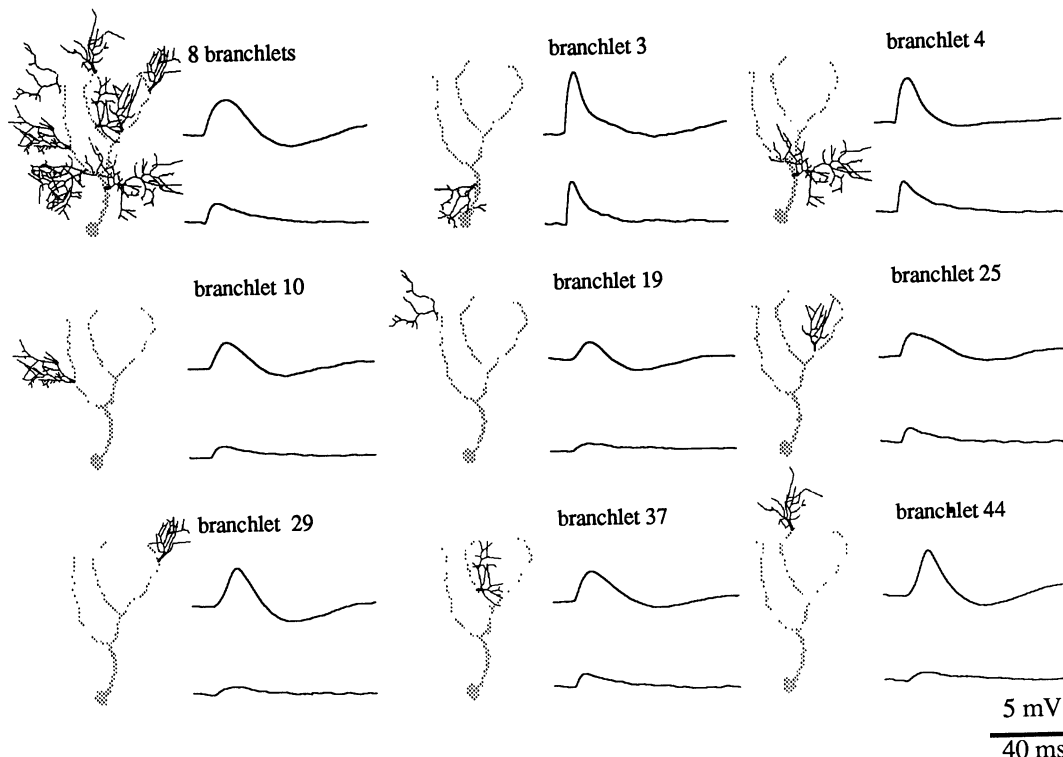


FIG. 1. Comparison of EPSPs generated by synchronous synaptic input at different locations in a model with active dendritic membrane and in a passive model. Each panel shows a gray schematic of the Purkinje cell, with the spiny branchlet(s) on which the synchronous input was delivered in black, and the corresponding somatic EPSP (average of eight traces) in the active membrane model (upper trace) and the passive membrane model (lower trace).

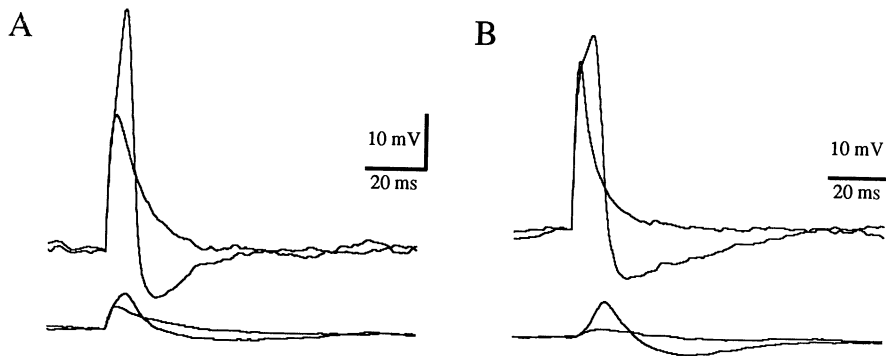


FIG. 3. EPSPs in spine heads (upper traces) and the soma (lower traces) with active and passive membrane models superimposed (average of eight traces). The EPSP in the passive membrane model was always lower in amplitude and peaked earlier. (A) Proximal input location (branchlet 4). (B) Distal input location (branchlet 44).

synaptic inputs were followed by a recruitment of P channels in other parts of the dendrite, surrounding the synaptic input (Fig. 4 C and F). This spread of P-channel activation caused additional depolarization of the dendrite but was insufficient to generate a full-blown dendritic spike. The increased current flow through P channels into the dendrite resulted in more somatic depolarization. Analysis of the model revealed that this P-channel activation in other parts of the dendrite occurred only in the presence of background parallel fiber inputs, which kept the dendrite at about  $-50$  mV (Fig. 4 A and G), close to the channel's activation threshold of  $-40$  mV (20, 21), so that small depolarizations caused by passive spread of the EPSP could partially activate the channels. Dendritic

$\text{Ca}^{2+}$ -activated  $\text{K}^+$  channels prevented the P-channel activation from generating a dendritic spike (11).

While synaptic inputs caused local activation of P channels everywhere in the dendrite, the geometry of the Purkinje cell made amplification less effective in proximal dendrites. In these regions, the current sink (2) caused by the large soma prevented the depolarization of proximal dendrites from spreading to adjacent branchlets, so that no additional P channels were recruited (Fig. 4 G-I).

Because of its dependence on P-channel activation, the amplification mechanism was sensitive to changes in the model parameters related to this channel. However, changes in P-channel densities of magnitudes that conserve the normal firing properties of the model (11) changed only the amplitude of amplification (Fig. 2), with lower densities causing a decreased amplification. Shifts of the P-channel activation threshold in the depolarizing direction progressively reduced the amplitude of amplification (Fig. 2), with a 7-mV shift resulting in no amplification at all.

The linear amplification mechanism made the number of somatic spikes fired after a synchronous input independent of dendritic location. Fig. 5 shows firing responses of the model, which are quite similar to experimental *in vivo* recordings of responses of Purkinje cells (22). There was a difference in timing of the response to proximal (Fig. 5B) versus distal (Fig. 5C) inputs, but the total number of spikes within 10 ms after the stimulus (solid bars in Fig. 5) was almost identical. The response within 10 ms is a standard measure of Purkinje cell responsiveness in the literature (23). The effect of dendritic location is shown in more detail in Table 1, which contains the average number of spikes within 10 ms of the synchronous input for 11 input locations and for different average firing frequencies of the model. Table 1 demonstrates that for each particular firing frequency there was  $<17\%$  difference in the number of spikes fired after inputs on different branchlets, within the entire physiological range of Purkinje cell firing frequencies [30–100 Hz (18)]. Furthermore, this consistency in response did not depend on clustering of the inputs on a single branchlet, as inputs distributed over eight branchlets gave similar responses. Note that while the amplification mechanism was robust for physiological firing frequencies of the model, it failed for unrealistic slow firing rates at or below 2 Hz. This failure at low frequencies was due to the inability of such low levels of spontaneous synaptic input to sufficiently depolarize the dendrite to enable P-channel activation.

## DISCUSSION

Shortly after  $\text{Ca}^{2+}$  channels were shown to generate spikes in Purkinje cell dendrites, Llinás and Sugimori (24) proposed that  $\text{Ca}^{2+}$  channels might amplify distal synaptic inputs by propagation of a spike along the dendrite from the input location to the soma. Similar mechanisms have been proposed in other neurons, including pyramidal neurons, where it has been suggested that dendritic  $\text{Na}^+$  and  $\text{Ca}^{2+}$  channels

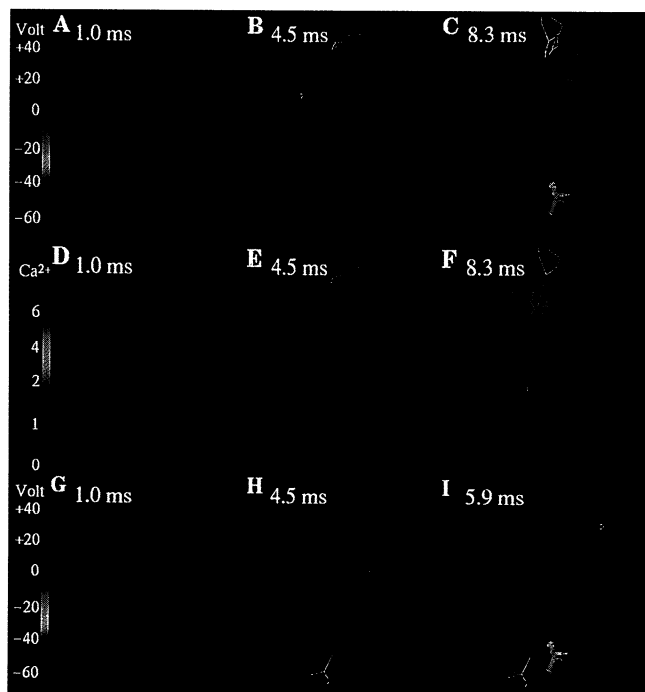


FIG. 4. False color images of the response of the Purkinje cell model to a synchronous synaptic input on a distal branchlet (branchlet 44; A-F) and a proximal branchlet (branchlet 3; G-I). See Fig. 1 for location and size of the branchlets. Membrane potential (A-C and G-I) and submembrane  $\text{Ca}^{2+}$  concentrations (D-F) at the times indicated after the input are shown. Initial depolarization at 1 ms was localized to the branchlet where the synaptic input was provided (A and G). For both inputs, P-channel activation (threshold at  $-40$  mV; colored green) had increased this local depolarization at 4.5 ms (B and H) and the resulting  $\text{Ca}^{2+}$  influx caused a sharp increase of the  $\text{Ca}^{2+}$  concentration (E). For distal input, surrounding parts of the dendrite were also depolarized (B) and by the time the neuron fired an action potential (C), P channels had activated in a large region surrounding input branchlet 44 (F). For proximal input, depolarization and P-channel activation were restricted to the original site of the synaptic input (I).

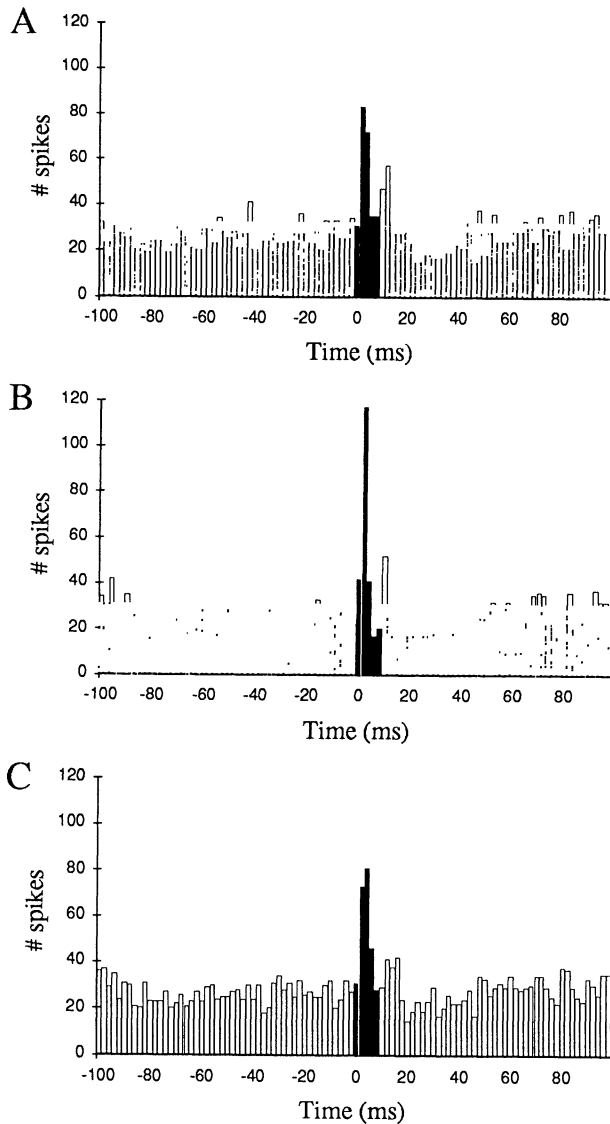


FIG. 5. Simulation of the change in spiking in response to a small synchronous synaptic input at different dendritic locations. (A) Peristimulus histogram (PST) for input distributed over eight branchlets. (B) PST for input on proximal branchlet 4. (C) PST for input on distal branchlet 37. PSTs were generated with 2-ms bins from 200 simulated trials.

(25, 26) might also amplify distant inputs by generation of dendritic spikes (27–29), by propagation of dendritic spikes to the soma (27), or by a subthreshold  $\text{Ca}^{2+}$ -dependent amplification (30).

While synaptic amplification by dendritic spikes has been proposed in several neurons, experimental evidence for such a mechanism is lacking. In Purkinje cells, dendritic spikes are found *in vivo* only in response to climbing fiber input (18, 31).

These cells do generate dendritic spikes in response to granule cell inputs *in vitro* (8); however, conditions of inhibition and excitation are sufficiently different in the slice preparation to produce very different kinds of dendritic behavior (12).

The amplification mechanism described in this paper does not depend on dendritic spike propagation. Amplification in the current model was dependent on the subspiking threshold activation of P channels in regions of the dendrite surrounding the synaptic input (Fig. 4). The resulting changes in membrane potential were small, especially in the smooth dendrites, which is consistent with physiological recordings (8). Other  $\text{Ca}^{2+}$  channels were not involved in the amplification mechanism, as the T-type channels (16) were almost completely inactivated at the dendritic membrane potentials measured in this study (Fig. 4A).

Because of the dependence of the amplification mechanism on a subspiking threshold recruitment of P channels, it is also gradual and “analog,” allowing it to be modulated by the electrotonic structure of the dendritic tree and resulting in an amplification that increases linearly with distance (Fig. 2). The more “digital” all-or-none mechanism of dendritic spike generation proposed by others (27–29) would almost certainly lack this property and therefore reintroduce a dependence on dendritic position and on clustering of synapses.

Other modeling studies have concluded that clustered synaptic inputs can provide more powerful inputs to pyramidal neurons than distributed ones (32, 33). However, this sensitivity to clustering could be explained by the voltage-dependent properties of *N*-methyl-D-aspartate (NMDA) receptor channels (33, 34). The adult Purkinje cell is the only large mammalian neuron that has no NMDA receptor channels (35). One functional consequence of the absence of NMDA receptors could thus be an insensitivity to clustering of synaptic inputs, suggesting that Purkinje cells might perform a fundamentally different computational task than pyramidal neurons.

The amplification results in our model were robust to small changes in P-channel density (Fig. 2) and to changes in background excitation (Table 1). Also, as the model was not specifically tuned to simulate synaptic responses (12), the amplification mechanism is an emergent property of the model. Our results are not contradicted by available physiological data, but direct experimental confirmation of this amplification mechanism may be difficult to obtain, because at present no procedures exist to apply localized, small inputs to the Purkinje cell dendritic tree *in vivo*. In principle, such an experiment could be designed *in vitro*; however, the model suggests that differential amplification of small inputs is dependent on the presence of continuous asynchronous parallel fiber inputs (Table 1). The slicing procedure greatly reduces this spontaneous input.

Some components of the amplification mechanism may have already been shown to exist experimentally. Facilitation of conduction of synaptic potentials by voltage-dependent responses has been reported in Purkinje cells (36) but was attributed to changes in electrotonic length, which seems

Table 1. Average number of spikes within 10 ms of a synchronous input applied to different dendritic branchlets

Excitation, Hz	Firing frequency, Hz	No. of spikes for inputs on branchlet										Input 8 branches
		2	4	6	10	14	19	25	29	37	44	
25	37.3	1.08	1.11	1.06	0.99	0.97	0.95	1.00	1.02	1.04	1.13	1.09
28	66.6	1.17	1.16	1.14	1.10	1.10	1.07	1.04	1.12	1.12	1.21	1.16
32	90.7	1.36	1.34	1.22	1.19	1.15	1.17	1.16	1.23	1.24	1.33	1.24
20	1.6	0.97	0.94	0.78	0.48	0.56	0.39	0.63	0.29	0.62	0.47	0.60

See Fig. 1 for location of branchlets. First column is average frequency of asynchronous excitation, and second column is resulting average firing frequency of the Purkinje cell model. Note that the number of spikes occurring in the absence of a stimulus can be computed by dividing the firing frequency by 100.

unlikely considering our modeling results (11). Several groups using high-resolution  $\text{Ca}^{2+}$  imaging methods *in vitro* have reported small, localized and rapidly changing increases in  $\text{Ca}^{2+}$  concentration during activation of parallel fiber inputs (ref. 39; A. Konnerth and T. Knöpfel, personal communication). These results show that massive parallel fiber inputs can cause localized changes in  $\text{Ca}^{2+}$  concentration comparable to the images shown in Fig. 4 E and F.

The relative insensitivity of a Purkinje cell to the location and clustering of dendritic inputs can be expected to have several functional implications. First, as has been pointed out by Marr (37), since a particular parallel fiber contacts all postsynaptic Purkinje cells at similar vertical dendritic locations (4), parallel fibers superficial in the molecular layer would otherwise have little overall effect on Purkinje cell output. Second, cerebellar development may be greatly simplified if the detailed pattern of connections onto individual Purkinje cells makes little difference. Establishing 150,000 connections to a single Purkinje cell (5) would be a formidable task if the precise position of each synapse was critical for function, especially because hundreds of Purkinje cells share inputs from the same parallel fiber (4). Finally, the amplification mechanism might provide Purkinje cells with the capacity to detect common features of synaptic input arising from different patterns of granule cell layer activity, which would activate distinct regions of the dendritic tree. Such patterns could, for example, be expected to arise from variations in inputs to the complex fractured maps of the body surface found in the tactile regions of the cerebellum (22, 38).

When the number of synaptic inputs received by the Purkinje cell is combined with the size and electrical complexities of its dendritic tree (6), this neuron is one of the most complex in the nervous system. The results presented here suggest that some of this cell's dendritic complexity may actually serve to simplify the development of its connections and the processing of its synaptic inputs. In this way, biophysical and anatomical complexity may subservise functional simplicity.

We thank M. Rapp, I. Segev, and Y. Yarom for reconstruction of the Purkinje cell and D. Jaeger and B. Mel for fruitful discussions. This research used the Intel Touchstone Delta System operated by California Institute of Technology on behalf of the Concurrent Supercomputing Consortium; U. S. Bhalla, D. Bilitch, and M. D. Speight helped in porting GENESIS to the Delta; and J. Leigh wrote the visualization software. E.D.S. was supported by Fogarty Fellowship F05 TW04368 (National Institutes of Health), and J.M.B. was supported by grants from the National Science Foundation (NS31378) and the National Institute of Neurological Disorders and Stroke (BIR-9017153).

- Rall, W. (1970) in *Excitatory Synaptic Mechanisms*, eds. Anderson, P. & Jansen, J. K. S. (Universiteto Forlaget, Oslo), pp. 175–187.
- Jack, J. J., Noble, D. & Tsien, R. W. (1975) *Electric Current Flow in Excitable Cells* (Clarendon, Oxford).
- Rall, W., Burke, R. E., Smith, T. G., Nelson, P. G. & Frank, K. (1967) *J. Neurophysiol.* **30**, 1169–1193.
- Palay, S. L. & Chan-Palay, V. (1974) *Cerebellar Cortex* (Springer, New York).
- Harvey, R. J. & Napper, R. M. A. (1991) *Prog. Neurobiol.* **36**, 437–463.
- Ito, M. (1984) *The Cerebellum and Neural Control* (Raven, New York).
- Miyakawa, H., Lev-Ram, V., Lasser-Ross, N. & Ross, W. N. (1992) *J. Neurophysiol.* **68**, 1178–1189.
- Llinás, R. R. & Sugimori, M. (1992) in *The Cerebellum Revisited*, eds. Llinás, R. R. & Sotelo, C. (Springer, Berlin), pp. 167–181.
- Bernander, Ö., Douglas, R. J., Martin, K. A. C. & Koch, C. (1991) *Proc. Natl. Acad. Sci. USA* **88**, 11569–11573.
- Rapp, M., Yarom, Y. & Segev, I. (1992) *Neural Comput.* **4**, 518–533.
- De Schutter, E. & Bower, J. M. (1994) *J. Neurophysiol.* **71**, 375–400.
- De Schutter, E. & Bower, J. M. (1994) *J. Neurophysiol.* **71**, 401–419.
- Rapp, M., Segev, I. & Yarom, Y. (1994) *J. Physiol. (London)* **474**, 87–99.
- Wilson, M. A., Bhalla, U. S., Uhley, J. D. & Bower, J. M. (1989) in *Advances in Neural Information Processing Systems*, ed. Touretzky, D. (Morgan Kaufmann, San Mateo, CA), pp. 485–492.
- Llinás, R. R., Sugimori, M., Lin, J. W. & Cherksey, B. (1989) *Proc. Natl. Acad. Sci. USA* **86**, 1689–1693.
- Kaneda, M., Wakamori, M., Ito, M. & Akaike, N. (1990) *J. Neurophysiol.* **63**, 1046–1051.
- Gruol, D. L., Jacquin, T. & Yool, A. J. (1991) *J. Neurosci.* **11**, 1002–1015.
- Llinás, R. R. (1981) in *Handbook of Physiology: The Nervous System II, Motor Control*, ed. Brooks, V. B. (Am. Physiol. Soc., Bethesda, MD), pp. 831–876.
- Gundappa-Sulur, G. & Bower, J. M. (1990) *Soc. Neurosci. Abstr.* **16**, 896.
- Regan, L. J. (1991) *J. Neurosci.* **11**, 2259–2269.
- Usovich, M. M., Sugimori, M., Cherksey, B. & Llinás, R. R. (1992) *Soc. Neurosci. Abstr.* **22**, 974.
- Bower, J. M. & Woolston, D. C. (1983) *J. Neurophysiol.* **49**, 745–766.
- Bloedel, J. R. (1992) *Behav. Brain Sci.* **15**, 666–678.
- Llinás, R. R. & Sugimori, M. (1979) *Prog. Brain Res.* **51**, 323–334.
- Benardo, L. S., Masukawa, L. M. & Prince, D. A. (1982) *J. Neurosci.* **2**, 1614–1622.
- Amitai, Y., Friedman, A., Connors, B. W. & Gutnick, M. J. (1993) *Cereb. Cortex* **3**, 26–38.
- Spencer, W. A. & Kandel, E. R. (1961) *J. Neurophysiol.* **24**, 272–285.
- Turner, R. W. & Meyers Der Barker, J. L. (1993) *Neuroscience* **53**, 949–959.
- Cauler, L. J. & Connors, B. W. (1992) in *Single Neuron Computation*, eds. McKenna, T., Davis, J. & Zornetzer, S. F. (Academic, Boston), pp. 199–229.
- Traub, R. D. & Llinás, R. R. (1979) *J. Neurophysiol.* **42**, 476–496.
- Armstrong, D. M. & Rawson, J. A. (1979) *J. Physiol. (London)* **289**, 425–448.
- Mel, B. (1992) *Neural Comput.* **4**, 502–517.
- Brown, H. T., Zador, A. M., Mainen, Z. F. & Claiborne, B. J. (1992) in *Single Neuron Computation*, eds. McKenna, T., Davis, J. & Zornetzer, S. F. (Academic, Boston), pp. 81–116.
- De Schutter, E. & Bower, J. M. (1993) *Neural Comput.* **5**, 681–694.
- Farrant, M. & Cull-Candy, S. G. (1991) *Proc. R. Soc. London B* **244**, 179–184.
- Llinás, R. R. & Sugimori, M. (1984) *Soc. Neurosci. Abstr.* **14**, 659.
- Marr, D. A. (1969) *J. Physiol. (London)* **202**, 437–470.
- Shambes, G., Gibson, J. M. & Welker, W. (1978) *Brain Behav. Evol.* **15**, 94–140.
- Midtgaard, J., Lasser-Ross, N. & Ross, W. N. (1993) *J. Neurophysiol.* **70**, 2455–2469.